



# Simultaneous blockade of VEGF and Dll4 by HD105, a bispecific antibody, inhibits tumor progression and angiogenesis

Dongheon Lee, Dongin Kim, Yu Bin Choi, Kyungjae Kang, Eun-Sil Sung, Jin-Hyung Ahn, Junseo Goo, Dong-Hoon Yeom, Hyun Sook Jang, Kyung Duk Moon, Sang Hoon Lee & Weon-Kyoo You

To cite this article: Dongheon Lee, Dongin Kim, Yu Bin Choi, Kyungjae Kang, Eun-Sil Sung, Jin-Hyung Ahn, Junseo Goo, Dong-Hoon Yeom, Hyun Sook Jang, Kyung Duk Moon, Sang Hoon Lee & Weon-Kyoo You (2016) Simultaneous blockade of VEGF and Dll4 by HD105, a bispecific antibody, inhibits tumor progression and angiogenesis, mAbs, 8:5, 892-904, DOI: [10.1080/19420862.2016.1171432](https://doi.org/10.1080/19420862.2016.1171432)

To link to this article: <http://dx.doi.org/10.1080/19420862.2016.1171432>

 View supplementary material [↗](#)

 Accepted author version posted online: 06 Apr 2016.  
Published online: 06 Apr 2016.

 Submit your article to this journal [↗](#)

 Article views: 97

 View related articles [↗](#)

 View Crossmark data [↗](#)

REPORT

## Simultaneous blockade of VEGF and Dll4 by HD105, a bispecific antibody, inhibits tumor progression and angiogenesis

Dongheon Lee, Dongjin Kim<sup>\*#</sup>, Yu Bin Choi<sup>\*</sup>, Kyungjae Kang<sup>\*</sup>, Eun-Sil Sung<sup>#</sup>, Jin-Hyung Ahn<sup>#</sup>, Junseo Goo, Dong-Hoon Yeom, Hyun Sook Jang, Kyung Duk Moon, Sang Hoon Lee<sup>#</sup>, and Weon-Kyoo You<sup>#</sup>

Hanwha Chemical R&D Center, Biologics Business Unit, Gajeong-Ro, Yuseong-Gu, Daejeon, Republic of Korea

### ABSTRACT

Several angiogenesis inhibitors targeting the vascular endothelial growth factor (VEGF) signaling pathway have been approved for cancer treatment. However, VEGF inhibitors alone were shown to promote tumor invasion and metastasis by increasing intratumoral hypoxia in some preclinical and clinical studies. Emerging reports suggest that Delta-like ligand 4 (Dll4) is a promising target of angiogenesis inhibition to augment the effects of VEGF inhibitors. To evaluate the effects of simultaneous blockade against VEGF and Dll4, we developed a bispecific antibody, HD105, targeting VEGF and Dll4. The HD105 bispecific antibody, which is composed of an anti-VEGF antibody (bevacizumab-similar) backbone C-terminally linked with a Dll4-targeting single-chain variable fragment, showed potent binding affinities against VEGF ( $K_D$ : 1.3 nM) and Dll4 ( $K_D$ : 30 nM). In addition, the HD105 bispecific antibody competitively inhibited the binding of ligands to their receptors, i.e., VEGF to VEGFR2 ( $EC_{50}$ :  $2.84 \pm 0.41$  nM) and Dll4 to Notch1 ( $EC_{50}$ :  $1.14 \pm 0.06$  nM). Using in vitro cell-based assays, we found that HD105 effectively blocked both the VEGF/VEGFR2 and Dll4/Notch1 signaling pathways in endothelial cells, resulting in a conspicuous inhibition of endothelial cell proliferation and sprouting. HD105 also suppressed Dll4-induced Notch1-dependent activation of the luciferase gene. In vivo xenograft studies demonstrated that HD105 more efficiently inhibited the tumor progression of human A549 lung and SCH gastric cancers than an anti-VEGF antibody or anti-Dll4 antibody alone. In conclusion, HD105 may be a novel therapeutic bispecific antibody for cancer treatment.

**Abbreviations:** ATCC, American Type Culture Collection; CHO, Chinese Hamster Ovary; CSCs, Cancer Stem Cells; DACE, Dual-Antigen Capture ELISA; DAPI, 4',6-Diamidino-2-phenylindole; DBZ, Dibenzazepine; Dll4, Delta-like ligand 4; HUVECs, Human Umbilical Vein Endothelial Cells; JCRB, Japanese Collection of Research Bioresources Cell Bank; NICD, Notch Intracellular Domain; PDX, Patient-Derived Xenograft; PIC, Protease and phosphatase Inhibitor Cocktails; rhDll4-His, His-tagged Recombinant Human Dll4; scFv, Single-Chain Fv; SEC-HPLC, Size Exclusion Chromatography-HPLC; TMB, 3,3',5,5'-Tetramethylbenzidine; VEGF, Vascular Endothelial Growth Factor; VEGFR, Vascular Endothelial Growth Factor Receptor

### ARTICLE HISTORY

Received 23 November 2015  
Revised 4 March 2016  
Accepted 21 March 2016

### KEYWORDS

Anti-angiogenesis; anti-cancer; biologics; delta-like ligand; therapeutic antibody; VEGF

### Introduction


Tumor angiogenesis, the formation of new blood vessels in solid tumors, contributes to tumor cell survival, growth and metastasis. An important driving force of tumor angiogenesis is the signaling pathway involving vascular endothelial growth factor (VEGF) and its receptors (VEGFRs).<sup>1</sup> Several angiogenesis inhibitors targeting the VEGF/VEGFR signaling pathway have been approved by the Food and Drug Administration, and are now used for the treatment of several cancers.<sup>2</sup> The first inhibitor of the VEGF/VEGFR signaling pathway to be approved was bevacizumab (Avastin<sup>®</sup>, Genentech/Roche), a monoclonal antibody against the human VEGF ligand.<sup>2</sup> The other protein-based inhibitors are ramucirumab (Cyramza<sup>®</sup>, Eli Lilly), a human monoclonal antibody against human

VEGFR, and aflibercept (VEGF-Trap; Eylea<sup>®</sup>, Regeneron).<sup>3,4</sup> Another class of inhibitors includes sunitinib (Sutent<sup>®</sup>, Pfizer) and sorafenib (Nexavar<sup>®</sup>, Bayer), which are small-molecule compounds that directly inhibit the phosphorylation of VEGFRs.<sup>2</sup> VEGF/VEGFR signaling inhibitors can block VEGF-driven angiogenesis and regress tumor vessels that are dependent on VEGF. However, VEGF inhibitors alone do not destroy all blood vessels in tumors. In addition, several pre-clinical studies have shown that VEGF inhibitors alone resulted in a more invasive pattern of tumors. Recently, a similar pattern of tumor infiltration has been observed in cancer patients as a result of resistance to anti-VEGF therapy.<sup>5-8</sup> Because those cancer patients are refractory to anti-angiogenic therapies, there is a strong clinical need for next-generation

**CONTACT** Weon-Kyoo You  weonkyoo.you@hanwha.com; weonkyoo.you@gmail.com; Sang Hoon Lee PhD.  sanghoon.lee@hanwha.com; wincancer@yahoo.com

<sup>\*</sup>These authors equally contributed to this work.

<sup>#</sup>Present affiliation: ABL Bio, Gajeong-Ro, Yuseong-Gu, Daejeon, Republic of Korea

 Supplemental data for this article can be accessed on the publisher's website.

© 2016 Hanwha Chemical

angiogenesis inhibitors to overcome resistance to anti-VEGF therapy.<sup>9,10</sup>

Delta-like ligand 4 (Dll4), a Notch ligand, also plays an important role in vascular development.<sup>11</sup> Although many genes are involved in vascular development, aside from the VEGF gene, Dll4 is the only gene whose haploinsufficiency leads to major vascular defects and embryonic lethality.<sup>11</sup> The Dll4/Notch signaling pathway regulates not only embryonic vasculature, but also tumor angiogenesis.<sup>11-13</sup> In particular, Dll4 is highly expressed in many human cancers, including kidney cancers, gastric cancers, lung cancers, bladder cancers, pancreatic cancers, colorectal cancers, and breast cancers.<sup>14,15</sup> Several preclinical xenograft studies have shown that Dll4/Notch blockade inhibited tumor progression by promoting the hyperproliferation of endothelial cells, which resulted in an increase in vascular density but a decrease in functional patent tumor vasculature.<sup>16-20</sup> In addition to the effects of Dll4 blockade on tumor vasculature, Dll4/Notch inhibition is known to reduce cancer stem cells (CSCs), which are an important cancer cell population for malignant tumor progression.<sup>21</sup> Therefore, Dll4 is now recognized as a promising target for improved efficacy in cancer treatment. Moreover, the Dll4/Notch signaling pathway acts as a key negative regulator downstream of the VEGF/VEGFR signaling pathway.<sup>14,15</sup> VEGF signaling activates the Notch pathway locally through the upregulation of Dll4 expression. Then, Dll4-dependent Notch activation leads to the suppression of the VEGF signaling pathway by the downregulation of VEGFR2 expression, resulting in the inhibition of excessive vessel branching by preventing endothelial tip cell formation.<sup>15</sup> This crosstalk between VEGF/VEGFR2 and Dll4/Notch signaling pathways suggests that the simultaneous blockade of both signaling pathways would provide improved efficacy for the inhibition of tumor progression and angiogenesis.<sup>14-16,19,20</sup>

We developed the HD105 bispecific antibody, targeting both VEGF and Dll4, as a potent anti-cancer therapeutic antibody. We generated HD105 by linking each C-terminal of an anti-VEGF antibody (bevacizumab-similar) with a Dll4-binding single-chain variable fragment (scFv).<sup>22,23</sup> The bevacizumab-similar, a biosimilar molecule from Hanwha Chemical, has the same complementarity-determining region sequence, and similar biological activity and cross-reactivity compared with the originator's molecule. In this report, we evaluate the *in vitro* activities of the HD105 bispecific antibody compared to a VEGF-targeting antibody (bevacizumab-similar) and a Dll4-targeting antibody alone. HD105 bound to both targets, VEGF and Dll4, with nanomolar  $K_D$  values, and dose-dependently inhibited VEGF/VEGFR and Dll4/Notch interaction. These biochemical activities of the bispecific antibody led to the potent inhibition of each signaling pathway in endothelial cells and the dose-dependent suppression of VEGF-induced or Dll4-induced cellular responses. In addition, we found that simultaneous blockade by the HD105 bispecific antibody inhibited the tumor progression of human A549 lung and SCH gastric cancers in xenograft models more effectively than a VEGF-targeting antibody (bevacizumab-similar) and a Dll4-targeting antibody alone. These results suggest that HD105 has promise as an anti-cancer therapeutic antibody to overcome resistance to anti-VEGF therapies.

## Results

### Simultaneous binding of HD105 bispecific antibody to VEGF and Dll4

The bispecific antibody HD105 is composed of a VEGF-targeting bevacizumab-similar IgG backbone and a Dll4-targeting single-chain Fv (Fig. 1A). To determine the binding affinities of HD105 against each target antigen, we performed Biacore assays and enzyme-linked immunosorbent assays (ELISAs) using the immobilized antigens VEGF and Dll4. The  $K_D$  value of HD105 (0.13 nM) against human VEGF was found to be 2-fold higher than the  $K_D$  value of the anti-VEGF bevacizumab-similar antibody (0.06 nM) in the Biacore assay (Fig. 1B). In addition, the  $K_D$  value of HD105 against human Dll4 (30 nM) was 10-fold higher than the  $K_D$  value of the anti-Dll4 monoclonal antibody (3.6 nM) (Fig. 1B). The higher  $K_D$  value of HD105 against human VEGF and Dll4 might be due to a difference in the structure of the antibody molecule between a conventional IgG and the bispecific format of the HD105 antibody.<sup>24,25</sup> Using ELISAs, we determined the dose-dependent binding profiles of the HD105 bispecific antibody against immobilized VEGF and Dll4 (Fig. 1C, 1D, respectively). The results of dual-antigen capture ELISA confirmed that each binding part of HD105 is actively maintained in the format of an IgG backbone linked with a scFvs (Fig. 1E). These results demonstrated that the binding affinity and kinetics of the bispecific antibody were comparable to the values for each single-antigen-targeting antibody.

Next, we determined whether the HD105 bispecific antibody inhibited the receptor-ligand bindings of VEGF/VEGFR2 and Dll4/Notch1. As shown in Fig. 1F, HD105 inhibited the interaction between human VEGF and human VEGFR2 (KDR) in a dose-dependent manner. The  $EC_{50}$  (half maximal effective concentration) value of HD105 in inhibiting VEGF/VEGFR-2 interaction was 2.84 nM, which is comparable with the  $EC_{50}$  value of the anti-VEGF (bevacizumab-similar) antibody (2.98 nM) (Fig. 1F). HD105 also inhibited the interaction between human Dll4 and Notch1. The  $EC_{50}$  value (1.14 nM) of HD105 was 2-fold higher than the  $EC_{50}$  value (0.65 nM) of the anti-Dll4 antibody (Fig. 1G), which might be due to the 10-fold lower binding affinity of Dll4 scFv in the bispecific antibody. Nonetheless, the results of competition inhibition ELISAs confirmed that the HD105 bispecific antibody effectively bound to each target and competitively inhibited the interaction of VEGF/VEGFR2 and Dll4/Notch1.

### Inhibition of VEGF- and Dll4-mediated signaling pathways and cell responses

To address the *in vitro* biochemical and biological activities of HD105, we examined the activation of downstream molecules of the VEGF/VEGFR2 or Dll4/Notch1 signaling pathways and signaling-mediated cellular responses after HD105 treatment. First, we determined the effects of the HD105 bispecific antibody on both signaling pathways, VEGF/VEGFR2 and Dll4/Notch1, in HUVECs (Fig. 2A). VEGF-induced VEGFR2 activation was monitored by the phosphorylation status of VEGFR2 and ERK (Fig. 2A, lanes 1-3), whereas the

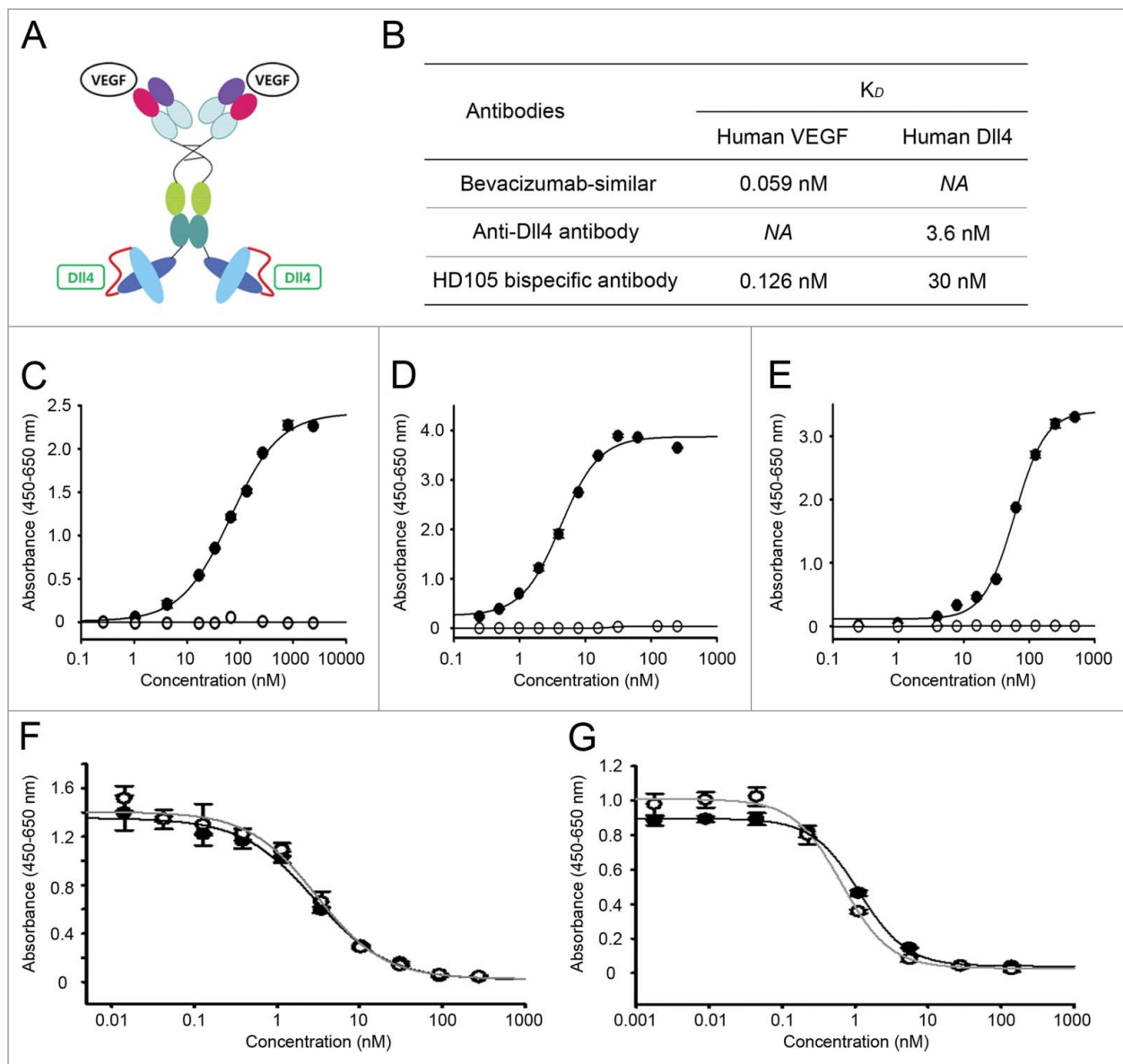


**Figure 1.** Simultaneous binding to VEGF and Dll4 by HD105 bispecific antibody leads to effective blockade of VEGF/VEGFR2 and Dll4/Notch1 interactions. The HD105 bispecific antibody was constructed of the C-terminal of the anti-VEGF (bevacizumab-similar) IgG backbone linked with a single-chain Fv targeting Dll4 (A). The binding affinity of the HD105 bispecific antibody against human VEGF or human Dll4 was determined by Biacore assays (B) and ELISAs (C, D). The  $K_D$  values of each antibody against VEGF or Dll4 are summarized in Table (B). The HD105 bispecific antibody (closed circle) dose-dependently bound to human VEGF (C) or Dll4 (D). In addition, the HD105 bispecific antibody simultaneously bound to each antigen, human VEGF and human Dll4, in dual-antigen capture ELISAs (E). The anti-Dll4 antibody (open circle in C) or the anti-VEGF (bevacizumab-similar) antibody (open circle in D, E) was used as negative control. Competitive ELISAs demonstrated that the HD105 bispecific antibody inhibited the interaction between VEGF/VEGFR2 (F) or Dll4/Notch1 (G) in a dose-dependent manner. The  $EC_{50}$  (half maximal effective concentration) values of the anti-VEGF (bevacizumab-similar) antibody (open circle) and HD105 bispecific antibody (closed circle) for VEGF/VEGFR2 inhibition were  $2.98 \pm 0.5$  nM and  $2.84 \pm 0.41$  nM, respectively (F). The  $EC_{50}$  values of the anti-Dll4 antibody (open circle) and HD105 bispecific antibody (closed circle) were  $0.65 \pm 0.06$  nM and  $1.14 \pm 0.06$  nM, respectively (G).

Dll4-mediated Notch signaling pathway was monitored by the induction of the Notch intracellular domain (NICD, Fig. 2A, lanes 4–6). The VEGF-induced VEGFR2 signaling pathway was completely suppressed by treatment with the anti-VEGF (bevacizumab-similar) antibody (Fig. 2A, lanes 3 and 6). The VEGF/VEGFR2 signaling pathway in HUVECs was also inhibited by treatment with HD105, but not by treatment with anti-Dll4 antibody or DBZ (dibenzazepine), a chemical inhibitor of Notch receptor (Fig. 2A, lanes 7–9). In the case of Dll4-mediated NICD induction, the Dll4-induced Notch1 signaling pathway was effectively inhibited by treatment with the HD105 bispecific antibody, anti-Dll4 antibody

or DBZ (Fig. 2A, lanes 7–9), but not by anti-VEGF (bevacizumab-similar) antibody (Fig. 2A, lane 6). These results demonstrated that the HD105 bispecific antibody simultaneously inhibited the downstream signaling pathways of both VEGF-VEGFR2 and Dll4-Notch1 in the endothelial cells.

Because VEGF-induced VEGFR2 activation eventually stimulates endothelial cell responses, we tested whether the HD105 bispecific antibody inhibits VEGF-induced HUVEC sprouting and proliferation compared to the anti-VEGF bevacizumab-similar antibody and anti-Dll4 antibody. To examine the effects on endothelial cell sprouting, HUVECs were

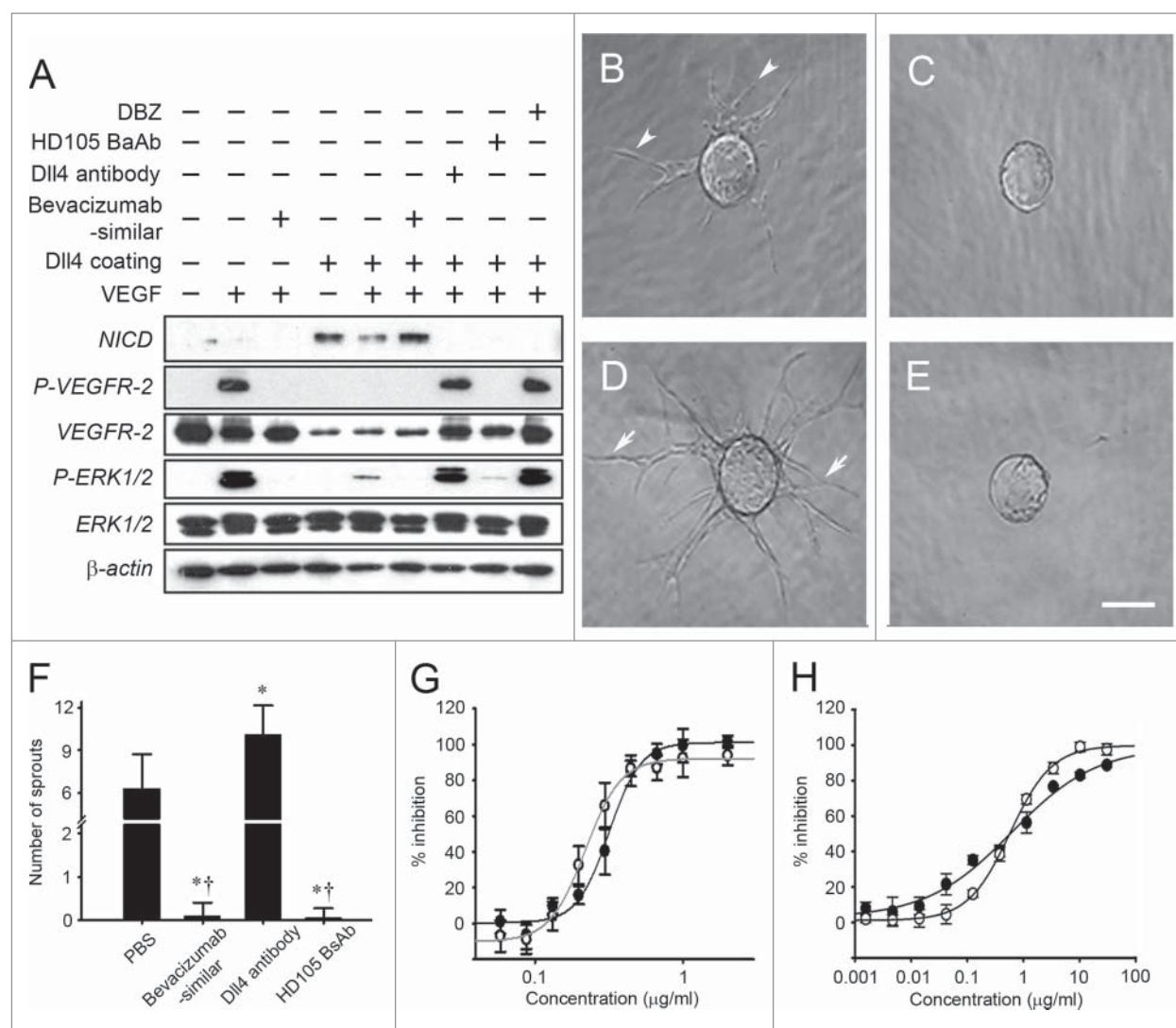


**Figure 2.** Blockade of both VEGF/VEGFR2 and Dll4/Notch1 signaling pathways by HD105 bispecific antibody leads to inhibition of each signaling-induced cellular response. The HD105 bispecific antibody inhibited both the VEGF/VEGFR2 and the Dll4/Notch1 signaling pathways in HUVECs (A). The VEGF/VEGFR2 signaling pathway was monitored by the activation of VEGFR2 and ERK (phosphorylation). The Dll4/Notch1 signaling pathway was monitored by the generation of NICD (Notch-induced intracellular domain). HUVEC sprouting assays were performed in a fibrin gel in the presence of PBS (B), anti-VEGF (bevacizumab-similar) antibody (C), anti-Dll4 antibody (D), or HD105 bispecific antibody (E). Representative images show sprouting tip cells of HUVECs from the beads under basal media (B, arrowheads) and more sprouting under anti-Dll4 antibody treatment (D, arrows) but much less sprouting under anti-VEGF antibody (C) or HD105 bispecific antibody treatment (E). Scale bar (B-E), 150 μm. The bar graph (F) shows the measurement of sprouting HUVECs at 225 μm from beads (n = 20 beads/group, mean ± SE). \*, P < 0.05 versus PBS. †, P < 0.05 vs. anti-Dll4 antibody. The HD105 bispecific antibody inhibited VEGF-dependent HUVEC proliferation (G) and Dll4-induced Notch-1-dependent activation of luciferase in SKOV-3-RBP-J<sub>κ</sub> luciferase cells (H) in a dose-dependent manner. The IC<sub>50</sub> values of the anti-VEGF (bevacizumab-similar) antibody (open circle) and HD105 bispecific antibody (closed circle) on HUVEC proliferation were 1.49 ± 0.04 nM and 1.58 ± 0.08 nM, respectively (G). The IC<sub>50</sub> values of the HD105 bispecific antibody (closed circle) and the anti-Dll4 antibody (open circle) on luciferase activation were determined to be 0.62 ± 0.23 nM and 0.58 ± 0.03 nM, respectively (H).

mixed with dextran-coated beads in fibrin gels, and then allowed to sprout under normal endothelial cell culture conditions (Fig. 2B). The sprouting endothelial tip cells were completely decreased after anti-VEGF (bevacizumab-similar antibody) treatment, but markedly increased after anti-Dll4 monoclonal antibody treatment compared to the control (Fig. 2C, D). In addition, the sprouting endothelial cells were decreased after HD105 bispecific antibody treatment (Fig. 2E). The measurement of the sprouting HUVECs at a certain distance (225 μm) from the beads showed a 49% increase after anti-Dll4 monoclonal antibody treatment, but an 89% decrease after treatment with anti-VEGF bevacizumab-similar antibody or HD105 bispecific antibody compared to the control (Fig. 2F).

In the case of endothelial cell proliferation, the HD105 bispecific antibody inhibited VEGF-induced HUVEC proliferation in a dose-dependent manner (Fig. 2G). The IC<sub>50</sub> value of HD105 was determined to be 1.58 ± 0.08 nM, which is comparable with the value of anti-VEGF antibody (1.49 ± 0.04 nM). To test the effects of HD105 on Dll4-mediated cell responses, we used engineered SKOV3 cancer cells expressing a luciferase gene regulated by Notch1 activation. HD105 dose-dependently inhibited Dll4-induced Notch1-dependent activation. The IC<sub>50</sub> value of HD105 was determined to be 0.62 ± 0.23 nM and the IC<sub>50</sub> value of the anti-Dll4 monoclonal antibody was 0.58 ± 0.03 nM, respectively (Fig. 2H). Based on the results of cell-based potency assays, we confirmed that the HD105 bispecific antibody suppressed cellular responses stimulated by either VEGF or Dll4.

### Suppression of tumor progression in xenograft models

To determine the effects of the HD105 bispecific antibody on tumor progression in vivo, we used human cancer xenograft models in nude mice treated with a mouse surrogate Dll4 antibody because VEGF was secreted by human cancer cells, whereas Dll4 was expressed by tumor endothelial cells originating from mice. We generated a mouse surrogate Dll4 antibody binding to the N-terminal regions of mouse Dll4 using similar binding epitopes to the N-terminal human Dll4 for the HD105 antibody (Fig. S1A-C). Thus, the mouse surrogate HD105 bispecific antibody can inhibit tumor progression via the neutralization of human cancer-secreted VEGF and host-expressed mouse endothelial Dll4 in xenograft models. Both mouse Dll4-targeting bispecific antibody and monoclonal antibody competitively inhibited the interaction of mouse Dll4/Notch1 with a similar range of  $EC_{50}$  values (Fig. S1C). In addition, the concentration of the mouse HD105 bispecific antibody was maintained at 83.3% after 100 hours of incubation at 37°C and the concentration of the mouse Dll4 antibody was maintained at 78.2% after 100 hours in mouse serum, respectively. In order to further evaluate the in vivo systemic exposure of HD105 and anti-Dll4 monoclonal antibody, we determined pharmacokinetic (PK) profiles and parameters of HD105 and anti-Dll4 antibody using BALB/c mice. We found no significant

differences in the PK profiles and parameters of HD105 compared to those of anti-Dll4 antibody (Fig. S1D, E). These results from mouse PK studies demonstrated that our bispecific antibody format has similar in vivo exposure and clearance patterns to Dll4-targeting monoclonal antibody.

In A549 human lung cancer xenograft models (Fig. 3A), the mouse surrogate HD105 bispecific antibody suppressed tumor progression more effectively (74%) than single-targeting antibodies, anti-VEGF bevacizumab-similar antibody alone (50%) or anti-mouse Dll4 antibody alone (50%). Similarly, the mouse surrogate HD105 bispecific antibody exhibited more potent effects on tumor progression inhibition (89%) than anti-VEGF bevacizumab-similar antibody alone (50%) or anti-mouse Dll4 antibody alone (50%) in SCH human gastric cancer xenograft models (Fig. 3B). In addition, the mouse surrogate HD105 bispecific antibody demonstrated a dose-dependent inhibition of tumor progression in SCH gastric cancer xenograft models (Fig. 3C). These in vivo results indicated that the simultaneous blockade of VEGF and Dll4 by the mouse surrogate HD105 bispecific antibody more potently suppressed tumor progression than each single-target antibody alone.

We then further investigated the effects of the mouse surrogate HD105 bispecific antibody on the tumor progression of other human gastric cancers such as MKN-74, SNU-5, and SNU-16. Although no significant effect on MKN-74 or SNU-5 tumor progression was observed (Fig. 3D, E), the mouse

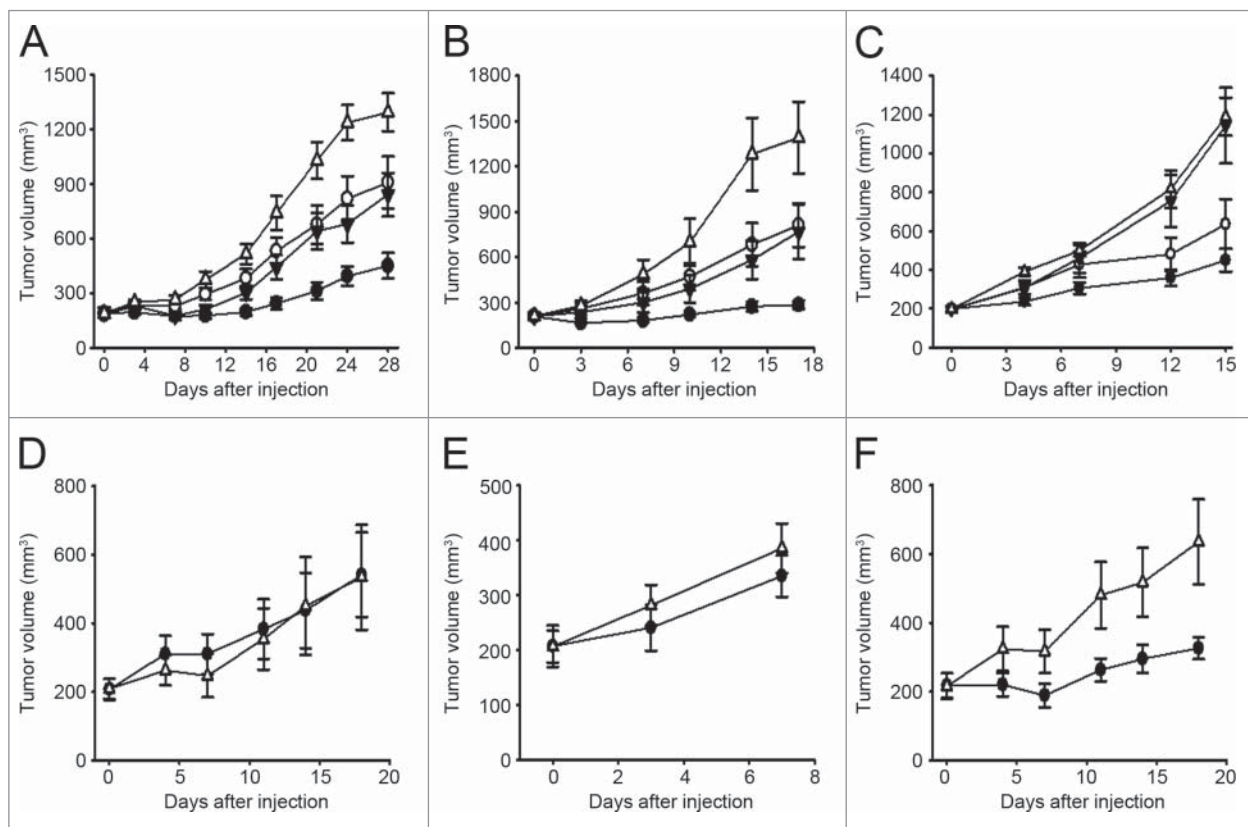


**Figure 3.** Suppression of tumor progression in several cancer xenograft models by HD105 bispecific antibody. Human A549 lung cancer (A) or human SCH gastric cancer (B, C) was subcutaneously implanted into nude mice. After tumors were grown to an average volume of 150–200 mm<sup>3</sup>, PBS (open triangle), anti-VEGF (bevacizumab-similar) antibody (2.5 mg/kg, open circle), anti-mouse Dll4 antibody (2.5 mg/kg, closed triangle), or mouse HD105 bispecific antibody (3.25 mg/kg, closed circle) was intraperitoneally injected twice (A549) or once (SCH) per week (A, B). Tumor volume was calculated by the formula width<sup>2</sup> × length × 0.52. The dose dependency of the mouse HD105 bispecific antibody was evaluated in human SCH gastric cancer xenograft model (C). PBS (open triangle) or mouse HD105 bispecific antibody (0.361 mg/kg, closed triangle; 1.083 mg/kg, open circle; 3.25 mg/kg, closed circle) was intraperitoneally injected once per week. The response to mouse HD105 bispecific antibody (6.5 mg/kg, once per week, closed circle) was also determined using other human gastric cancer xenograft models, including MKN-74 (D), SNU-5 (E), and SNU-16 (F). Tumor progression was not inhibited by the mouse HD105 bispecific antibody in MKN-74 and SNU-5 but was inhibited in SNU-16 similarly to SCH.

surrogate HD105 bispecific antibody inhibited SNU-16 tumor progression by 50%, a similar level to the findings in the SCH xenograft model (Fig. 3F).

### Effects on tumor vessels and tumor cells

To investigate the effects of the simultaneous blockade of VEGF and Dll4 on tumor vessels, we performed immunohistochemical

analysis of A549 and SCH tumor tissues after treatment with each antibody. The endothelial cells of tumor vessels, vascular basement membrane, and pericytes were stained for CD31, type IV collagen, and NG2, respectively. After treatment with the anti-VEGF (bevacizumab-similar) antibody or the mouse surrogate HD105 bispecific antibody, CD31-positive tumor vessels were reduced in A549 tumors compared to tumor vessels treated with phosphate-buffered saline (PBS) or the anti-mouse Dll4

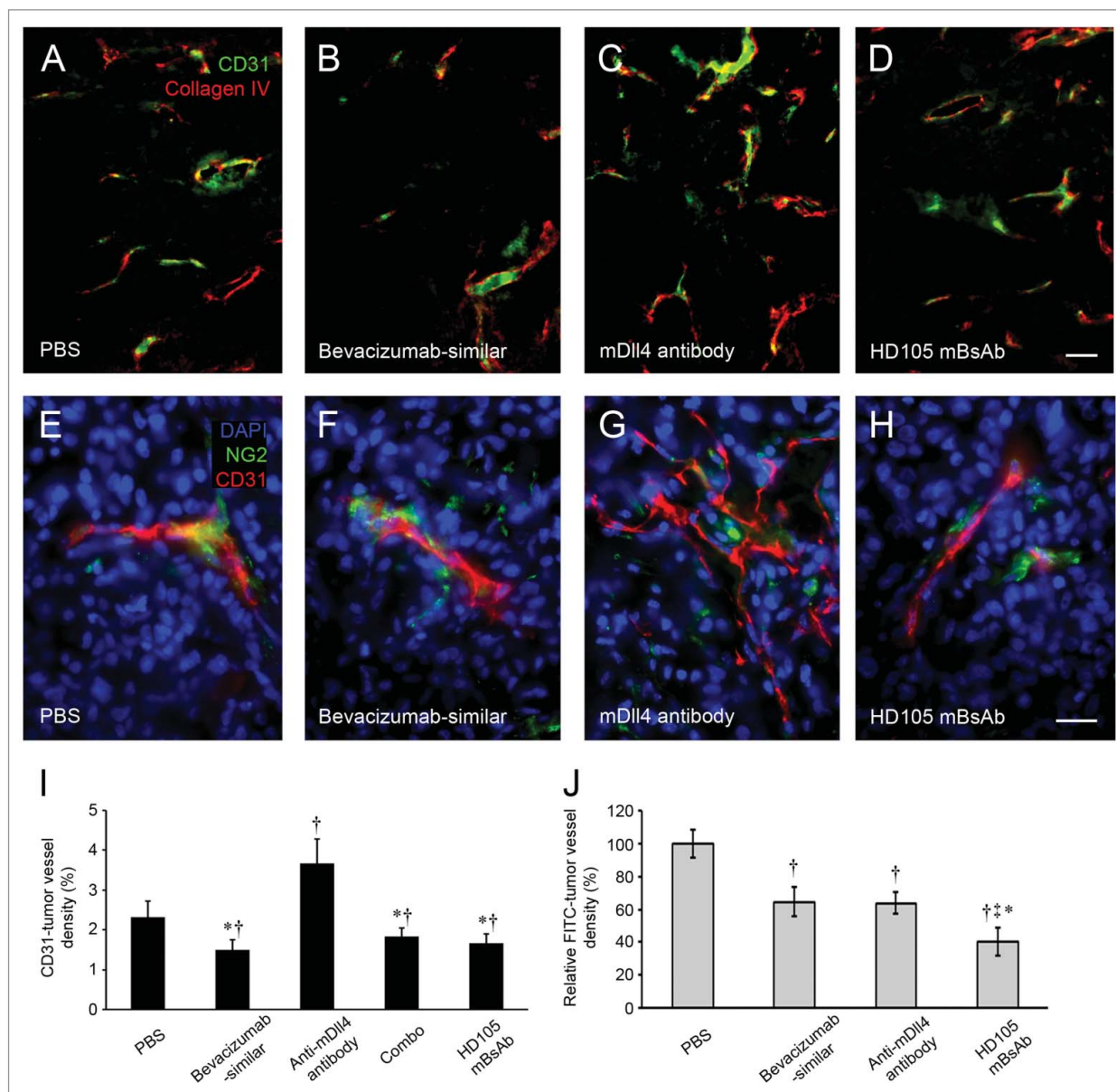


**Figure 4.** Suppression of tumor angiogenesis in cancer xenograft models by HD105 bispecific antibody. Fluorescence micrographs compare the vasculature of A549 human lung cancer tissues in xenograft mice after treatment with PBS (A), anti-VEGF (bevacizumab-similar) antibody (B), anti-mouse Dll4 antibody (C), or mouse HD105 bispecific antibody (D). Scale bar (A-D), 50  $\mu$ m. The tumor vasculature was stained for CD31 immunoreactivity (green), and the vascular basement was stained for type IV collagen (red). Tumor vessels were decreased after treatment with anti-VEGF (bevacizumab-similar) antibody or mouse HD105 bispecific antibody, whereas tumor vessels were markedly increased after treatment with anti-mouse Dll4 antibody compared to PBS. Higher-resolution images compare the phenotype changes of tumor vessels in detail after PBS (E), anti-VEGF (bevacizumab-similar) antibody (F), anti-mouse Dll4 antibody (G), or mouse HD105 bispecific antibody treatment (H). Scale bar (E-H), 20  $\mu$ m. The tumor vasculature was stained for CD31 immunoreactivity (red), and the perivascular pericyte was stained for NG2 (green). The nuclei of the tumor tissues were stained by DAPI (4',6-diamidino-2-phenylindole). Tumor vessels after treatment with anti-mouse Dll4 antibody were conspicuously thinner and more branched than the tumor vessels of other groups. Bar graph (I) measuring tumor vessel density of A549 tumor tissues in xenograft mice confirms the conspicuous increase of tumor vessels after anti-mouse Dll4 antibody treatment but decreases after anti-VEGF (bevacizumab-similar) antibody, mouse HD105 bispecific antibody, or combination treatment with anti-mouse Dll4 antibody and anti-VEGF (bevacizumab-similar) antibody. †,  $P < 0.05$  versus PBS. \*,  $P < 0.05$  vs. anti-Dll4 antibody. However, the functional tumor vessels in SCH gastric cancer tissues assessed by intravenous FITC-labeled *Lycopersicon esculentum* (Tomato) lectin staining were significantly decreased after treatment with anti-VEGF (bevacizumab-similar) antibody as well as anti-mouse Dll4 antibody (J). †,  $P < 0.05$  versus PBS. ‡,  $P < 0.05$  vs. anti-VEGF (bevacizumab-similar) antibody. \*,  $P < 0.05$  versus anti-Dll4 antibody. Functional tumor vessels were more decreased after treatment with mouse HD105 bispecific antibody compared to the other groups.

antibody alone (Fig. 4A-D). After treatment with anti-mouse surrogate Dll4 antibody, the tumor vessels had many more branches, but a thinner phenotype, compared to the tumor vessels of other groups in the fluorescence images under high magnification (Fig. 4E-H). Tumor vessel density was increased by 58% after treatment with the anti-mouse surrogate Dll4 antibody, whereas tumor vessel densities were reduced after treatment with the anti-VEGF bevacizumab-similar antibody (35%), the combination of the anti-VEGF (bevacizumab-similar) antibody plus the anti-mouse surrogate Dll4 antibody (21%), or the mouse surrogate HD105 bispecific antibody (28%) (Fig. 4I). We also found a similar level of changes in the tumor vessel densities of SCH tumor tissues (data not shown).

We then evaluated the effects of each antibody on functional tumor blood vessels in tumors by the intravenous injection of FITC-labeled *Lycopersicon esculentum* (tomato) lectin prior to the perfusion of mice used in the xenograft studies.<sup>9,10</sup> In the case of treatment with the anti-VEGF (bevacizumab-similar) antibody, functional tumor vessels in SCH tumors were reduced by 35%, which is a similar level of reduction in tumor vessel density (Fig. 4I, J). Compared to the conspicuous increase in tumor vessel density after treatment with the anti-mouse surrogate Dll4 antibody, functional patent tumor vessels were reduced by 36% in SCH tumors (Fig. 4I, J). More importantly, after treatment

with the mouse surrogate HD105 bispecific antibody, functional tumor vessels were reduced by 60% in SCH tumors compared to other groups (Fig. 4I, J). These results suggested that the simultaneous blockade of VEGF and Dll4 led to a significant reduction in both the density and the functionality of tumor vessels.

Because the results might be associated with tumor cell status, we assessed the status of apoptotic tumor cells using activated caspase-3 staining with DAPI nuclear staining. As shown in Fig. 5, apoptotic tumor cells stained by anti-activated caspase-3 antibody were significantly increased (by 2.4-fold) in SCH tumors after treatment with the mouse surrogate HD105 bispecific antibody compared to the PBS control group, the anti-VEGF (bevacizumab-similar) antibody or the anti-mouse Dll4 antibody group. Overall, the immunohistochemical studies demonstrated that treatment with the mouse surrogate HD105 bispecific antibody regressed tumor vessels, followed by the induction of apoptosis in tumor cells.

### Stability of HD105 bispecific antibody

The HD105 bispecific antibody was produced by Chinese hamster ovary (CHO) cells and then purified by several chromatographic steps. The purified HD105 bispecific antibody

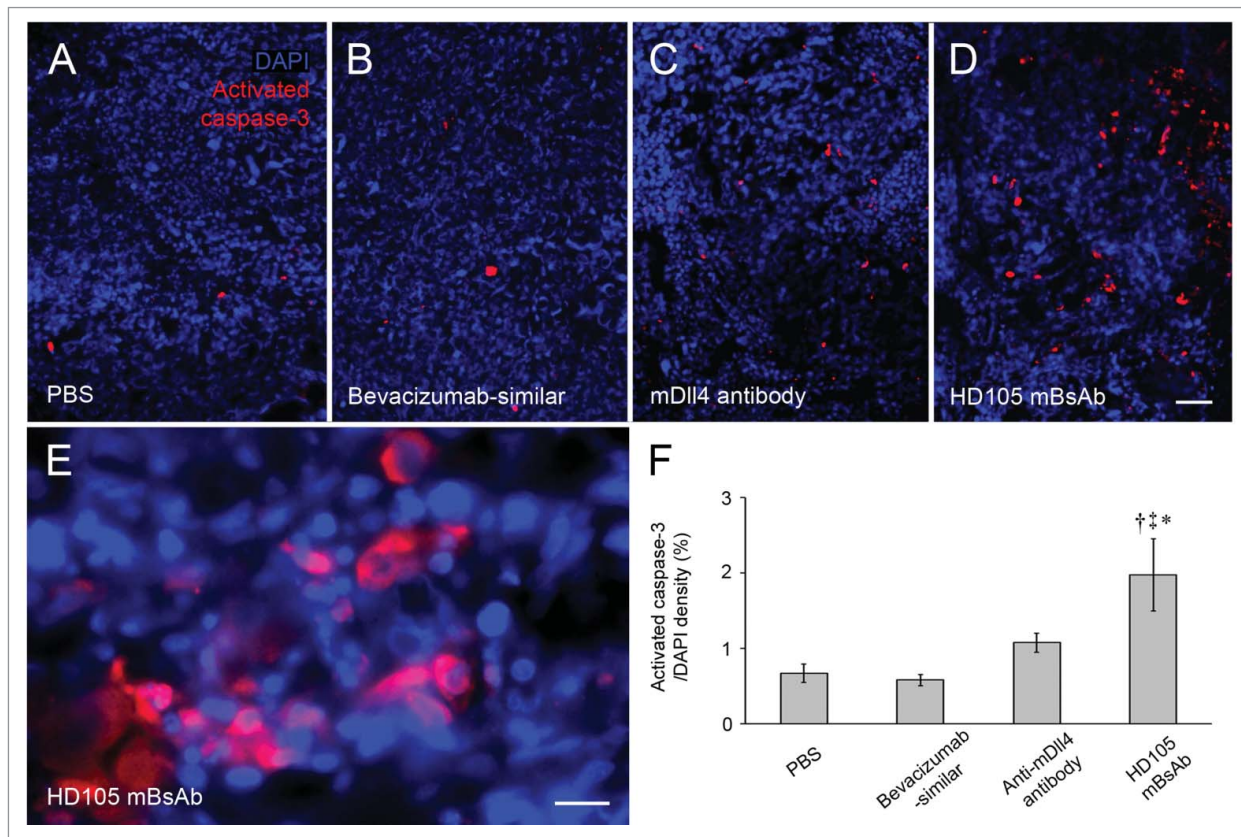


**Figure 5.** Increase in apoptotic tumor cells in cancer xenograft models treated with HD105 bispecific antibody. Fluorescence micrographs show apoptotic cells stained for activated caspase-3 antibody (red) in SCH human gastric cancer tissues in xenograft mice after treatment with PBS (A), anti-VEGF (bevacizumab-similar) antibody (B), anti-mouse Dll4 antibody (C), and mouse HD105 bispecific antibody (D and E). Scale bar (A-D), 50  $\mu$ m; (E), 20  $\mu$ m. Nuclei of the tumor tissues were stained by DAPI (4',6-diamidino-2-phenylindole, blue). The higher-resolution image confirms that activated caspase-3 antibody was stained in the cytoplasm of the apoptotic cells after mouse HD105 bispecific antibody treatment (E). The bar graph (F) measuring the cell density of apoptotic cells in SCH cancer tissues confirms the significant increase in apoptotic cells after mouse HD105 bispecific antibody treatment. \*,  $P < 0.05$  vs. PBS. †,  $P < 0.05$  versus anti-VEGF (bevacizumab-similar) antibody. ‡,  $P < 0.05$  vs. anti-Dll4 antibody.



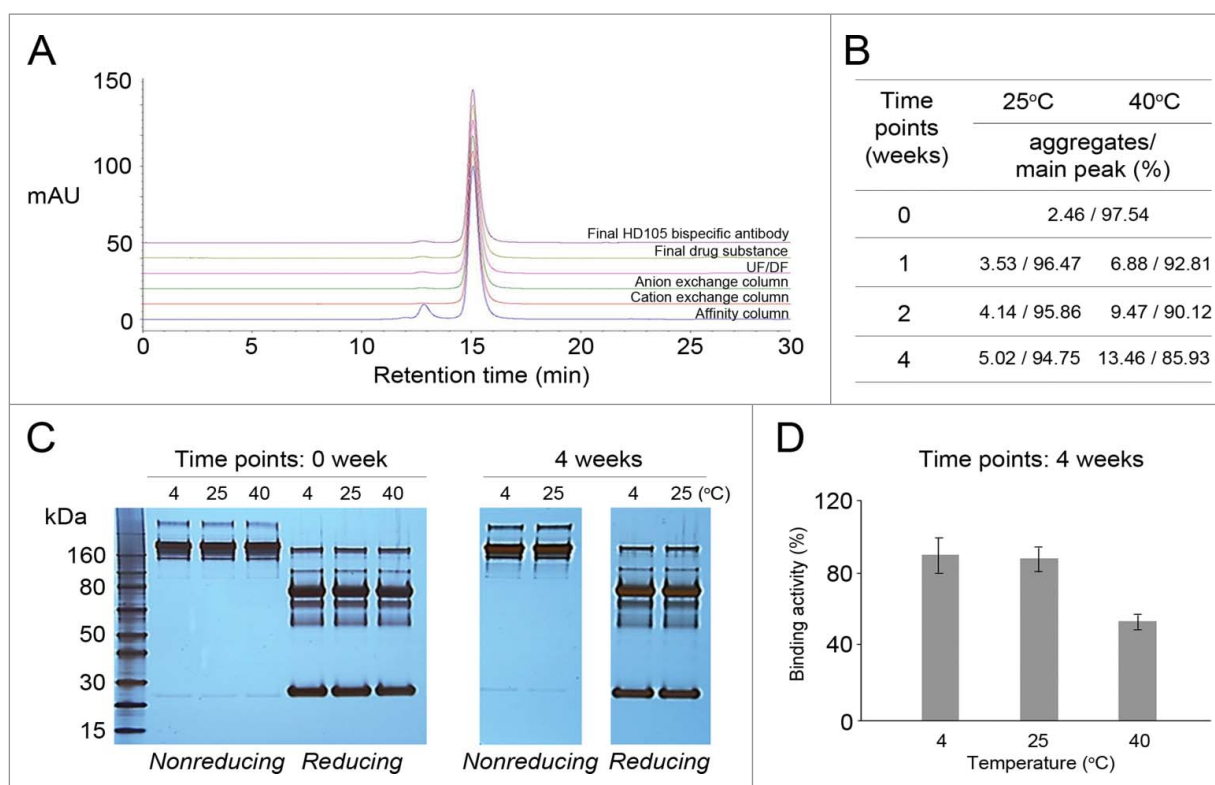


**Figure 6.** Purification and stability of HD105 bispecific antibody. The HD105 bispecific antibody was produced by CHO cells and then purified by several chromatographic steps. The purity of the antibody in each purification step was analyzed by SEC-HPLC (A). The stability of the purified HD105 bispecific antibody (20 mg/ml) was monitored by SEC-HPLC (B) and SDS-PAGE (C) after 4 weeks' incubation at 4°C, 25°C, or 40°C. The binding affinity against each target of the HD105 bispecific antibody was also monitored by DACE analysis (D) after 4 weeks' incubation at 4°C, 25°C, or 40°C.

contained less than 5% of aggregates by size-exclusion chromatography-high-performance liquid chromatography (SEC-HPLC) analysis, which might be the dimer fraction of the HD105 bispecific antibody (Fig. 6A). The stability of the HD105 bispecific antibody (20 mg/ml) was monitored by SEC-HPLC, SDS-PAGE, and dual-antigen capture ELISA (DACE) analysis after 4 weeks' incubation of the antibody at 4°C, 25°C, or 40°C (Fig. 6B-D). The monomer fraction and the binding affinity of the HD105 bispecific antibody were maintained within the acceptance criteria specified in each analysis after 4 weeks' incubation less than 25°C.

## Discussion

The goal of this study was to evaluate the *in vitro* and *in vivo* activity of the HD105 bispecific antibody targeting VEGF and Dll4, which are critical signaling mediators in tumor-induced angiogenesis. Several angiogenesis inhibitors that target the VEGF/VEGFR signaling pathway, including bevacizumab, ramucirumab, sunitinib and sorafenib, have been used for the treatment of cancer patients.<sup>1-3</sup> However, recent preclinical studies demonstrated that VEGF blockade alone led to a more invasive and aggressive pattern of tumors invading neighboring normal tissues, possibly due to increased intratumoral hypoxia.<sup>5-8</sup> Similar invasive and aggressive patterns of tumors were found in some cancer patients as a result of resistance to anti-VEGF therapy.<sup>5-8</sup> Therefore, additional targets of tumor-induced angiogenesis have been sought to overcome such

resistance to anti-VEGF therapies. Dll4, a Notch ligand, is another important signaling mediator in tumor angiogenesis.<sup>11</sup> Dll4 inhibitors have shown potent anti-tumor effects in a broad spectrum of cancer xenograft models, including models with intrinsic or acquired resistance to VEGF therapy.<sup>19,20,26</sup> Dll4 inhibitors were also shown to reduce cancer stem cell (CSC) frequency in several preclinical patient-derived cancer xenograft (PDX) models.<sup>21</sup> These emerging reports suggest that the Dll4/Notch signaling pathway might be a promising target for cancer treatment, with the possibility not only of inhibiting tumor angiogenesis, but also of reducing the CSC population. Moreover, combination treatment with VEGF and Dll4 inhibitors has demonstrated a more effective regression of tumor vessels and inhibition of tumor progression in several cancer xenograft models compared to VEGF or Dll4 blockade alone.<sup>14-20</sup>

Based on this scientific evidence, we developed HD105, a bispecific antibody that targets VEGF and Dll4 simultaneously. This bispecific antibody consists of an anti-VEGF bevacizumab-similar IgG backbone linked with a Dll4-binding single-chain Fv.<sup>22,23</sup> We note that a dual-targeting bispecific antibody against VEGF and Dll4, OMP-305B83, was developed and recently entered an ongoing Phase 1 study sponsored by OncoMed Pharmaceuticals.<sup>27,28</sup> Each arm of OMP-305B83, composed of two distinct heavy chains and a common light chain, binds to VEGF and Dll4, respectively.<sup>27,28</sup> Heterodimer formation of two distinct heavy chains is promoted by mutations at CH3 domain of Fc region. Compared to one binding site for each antigen in OMP-305B83, the HD105 bispecific antibody has two binding sites for each antigen (Fig. 1A).

We successfully expressed and purified the HD105 bispecific antibody from a CHO DG44 cell line. Then, we compared the *in vitro* biochemical properties and activities of the HD105 bispecific antibody with the properties of each single-antigen-targeting antibody, anti-VEGF bevacizumab-similar antibody or anti-Dll4 monoclonal antibody. The binding affinity of HD105 against VEGF was 2-fold weaker than for the anti-VEGF (bevacizumab-similar) antibody, whereas the affinity of HD105 against Dll4 was 10-fold weaker than for the anti-Dll4 antibody. This weaker binding affinity of the bispecific antibody might be due to the different conformation of the HD105 bispecific antibody compared to the general IgG antibody format. Generally, the binding affinity against a target antigen in a single-chain Fv format is much lower than the affinity in a conventional monoclonal IgG antibody format.<sup>24,25</sup> However, the HD105 bispecific antibody inhibited both receptor-ligand interactions, VEGF/VEGFR2 and Dll4/Notch1, with comparable EC<sub>50</sub> values to the anti-VEGF (bevacizumab-similar) antibody against VEGF/VEGFR2 and the anti-Dll4 monoclonal antibody against Dll4/Notch1. These *in vitro* biochemical activities of the HD105 bispecific antibody led to potent inhibition of both the VEGF/VEGFR-2 and Dll4/Notch1 signaling pathways in endothelial cells, endothelial cell sprouting and proliferation, and Dll4-induced Notch1-response in engineered SKOV-3 cells.

To address the *in vivo* efficacy of the HD105 bispecific antibody targeting VEGF and Dll4 in human-origin cancer xenograft models in mice, we used a mouse surrogate HD105 bispecific antibody because Dll4 is expressed by mouse endothelial cells in implanted human cancers. We found that the mouse surrogate HD105 bispecific antibody more effectively suppressed tumor progression in A549 lung cancer and SCH gastric cancer xenograft models compared to each single-antigen-targeting antibody, the anti-VEGF (bevacizumab-similar) antibody or the mouse surrogate Dll4-targeting antibody. Based on the results of immunohistochemical analysis, we also found that many more functional tumor vessels were regressed and more tumor cells were apoptotic after the simultaneous blockade of VEGF and Dll4. The greater regression of tumor vessels in response to the HD105 bispecific antibody was consistent with previous findings that Dll4 blockade enhances the anti-angiogenic effects of VEGF blockade after combination treatment.<sup>16,19</sup> These results suggested that the more potent suppression of tumor progression might be correlated with the regression of tumor vessels and induction of apoptotic tumor cells by the simultaneous blockade of VEGF and Dll4. However, the simultaneous blockade of VEGF and Dll4 by the HD105 bispecific antibody showed different anti-cancer effects in other human gastric cancer xenograft mouse models, including MKN-74, SNU-5, and SNU-16. These different anti-cancer effects of HD105 might be due to different contributions of the VEGF/VEGFR2 or the Dll4/Notch1 signaling pathway when each human gastric cancer cell is implanted into the mice.

To address this issue, we intend to investigate the expression levels of the proteins involved in the VEGF/VEGFR2 and Dll4/Notch1 signaling pathways using these gastric cancer xenograft tissues and cancer cell lines. We

expect that the expression profiles of VEGF/VEGFR2- and Dll4/Notch1-signaling pathway-related proteins will provide important clues for identifying a biomarker to determine which type of gastric cancer patients can be more effectively treated by the simultaneous blockade of VEGF and Dll4 in future clinical trials.

In conclusion, we found that the HD105 bispecific antibody targeting VEGF and Dll4 showed comparable activities to an anti-VEGF antibody (bevacizumab-similar) or an anti-Dll4 antibody in biochemical and biological *in vitro* assays. Furthermore, the HD105 bispecific antibody exhibited more potent *in vivo* efficacy in inhibiting the tumor progression of A549 and SCH human cancer xenografts than the VEGF or the Dll4 single-targeting antibody. These results suggest that the HD105 bispecific antibody might be a powerful anti-cancer therapeutic antibody for patients resistant to anti-VEGF therapies.

## Materials and methods

### Antibodies and cell culture

An anti-VEGF (bevacizumab-similar) antibody, an anti-Dll4 monoclonal antibody, the HD105 bispecific antibody, an anti-mouse Dll4 monoclonal antibody, and a mouse version of the HD105 bispecific antibody were produced by Hanwha Chemical, Biologics R&D Center (Daejeon, South Korea). The antibody targeting human Dll4 was screened by *in vitro* library/phage display methods using the OPAL library.<sup>29,30</sup> The anti-Dll4 monoclonal antibody is a fully human antibody that selectively binds to the N-terminal DSL domain of human Dll4. The HD105 bispecific antibody has a bevacizumab-similar IgG backbone, and the bevacizumab-similar C-terminal is linked with a single-chain Fv that binds to human Dll4.<sup>22,23</sup> The anti-mouse Dll4 monoclonal antibody was also screened and generated by *in vitro* phage display methods using the OPAL library,<sup>29,30</sup> which binds to the DSL domain of mouse Dll4. All antibodies were produced by CHO cells and then purified by several chromatographic steps for each antibody. All antibodies used in this study had over 95% purity.

Human umbilical vein endothelial cells (HUVECs, Lonza) were used for proliferation and sprouting assays. Detroit 551 cells (ATCC, American Type Culture Collection) were co-cultured with HUVECs in sprouting assays. SKOV-3 cancer cells (ATCC) were engineered to evaluate the activity on Dll4-induced cell response. A549 (ATCC), SCH (JCRB, Japanese Collection of Research Bioresources Cell Bank), MKN-74 (JCRB), SNU-5 (ATCC), and SNU-16 (ATCC) human cancer cells were used for *in vivo* mouse xenograft studies.

### Determination of binding affinities to VEGF and Dll4

To compare the binding affinities of the HD105 bispecific antibody with a bevacizumab-similar and an anti-Dll4 monoclonal antibody, a Biacore assay and an ELISA were performed as described below. Surface plasmon resonance experiments were performed using a Biacore T200 instrument (GE Healthcare) with HBS-EP buffer (GE Healthcare) at 25°C. Recombinant human VEGF (R&D Systems) and His-tagged recombinant

human Dll4 (rhDll4-His, R&D Systems) were immobilized on activated CM5 chip surfaces to  $\sim 100$  resonance units at a flow rate of  $30 \mu\text{l}/\text{min}$  using acetate buffer (GE Healthcare, pH 5.5). A flow cell without any antigens served as a reference surface. Responses were obtained by injecting various concentrations (6.25–100 nM, series of 2-fold dilutions) of anti-VEGF (bevacizumab-similar) antibody, anti-Dll4 monoclonal antibody or HD105 bispecific antibody over the flow cells at a rate of  $30 \mu\text{l}/\text{min}$  for 250 seconds, followed by dissociation in buffer for 600 seconds. The sensor chip surfaces were regenerated by injecting  $15 \mu\text{l}$  of glycine, pH 1.5 (GE Healthcare), at a rate of  $30 \mu\text{l}/\text{min}$  for 30 seconds. Kinetic data were analyzed with the Biacore T200 evaluation software version 1.0 and were fitted to a bivalent analyte model to determine the equilibrium dissociation constant  $K_D$  by measuring the ratio of the rate constants ( $K_D = k_d/k_a$ ).

ELISAs were performed in 96-well Nunc-Immuno MaxiSorp plates (Nalgene Nunc International) coated with recombinant human VEGF (50 ng/well) or anti-His Tag antibody (200 ng/well, R&D Systems) for 16 hours at  $4^\circ\text{C}$  and blocked with PBS containing 1% bovine serum albumin (BSA) for 2 hours at  $37^\circ\text{C}$ . For the Dll4-binding assay, His-tagged recombinant human Dll4 (rhDll4-His,  $2 \mu\text{g}/\text{ml}$ ) was captured on anti-histidine-coated plates by additional incubation for 1 hour at  $37^\circ\text{C}$ . After being washed with PBS-T (PBS containing 0.05% Tween 20, 5 times), various concentrations of HD105 bispecific antibody were added to each plate and then incubated for 2 hours at  $37^\circ\text{C}$ . After being washed with PBS-T four times, the bound antibodies were detected by incubation of a peroxidase-conjugated anti-human IgG Fab antibody (Pierce, 1:50,000) for 1 hour at  $37^\circ\text{C}$ . After additional washing,  $100 \mu\text{l}$  of 3,3',5,5'-tetramethylbenzidine (TMB) substrate reagent (Sigma) was added and incubated for 6 min. The reaction was stopped by adding  $50 \mu\text{l}$  of 1 N sulfuric acid, and the absorbance (450–650 nm) was measured using a microplate reader (Molecular Device SpectraMax 190, Tecan). Anti-VEGF antibody (bevacizumab-similar) and anti-Dll4 monoclonal antibody were used as a negative control for the Dll4-binding ELISA and for the VEGF-binding ELISA, respectively.

DACE was performed to confirm whether HD105 binds to both targets simultaneously. The plates were coated with recombinant human VEGF (25 ng/well) for 16 hours at  $4^\circ\text{C}$ . After blocking and washing, various concentrations of HD105 bispecific antibody were mixed with an equal volume of rhDll4-His ( $2 \mu\text{g}/\text{ml}$ ). The mixtures of the bispecific antibody and rhDll4-His were transferred to the VEGF-coated wells and incubated for 2 hours at  $37^\circ\text{C}$ . After being washed with PBS-T, the bound rhDll4-His was detected by peroxidase-conjugated anti-His6 antibody (Roche, 1:1,000) for 1 hour at  $37^\circ\text{C}$ . The detection procedures of the reaction were the same as for the above-described ELISA method. Anti-VEGF antibody (bevacizumab-similar) or anti-Dll4 monoclonal antibody was used as a negative control for the DACE.

### **Inhibition of receptor-ligand bindings**

To determine whether HD105 bispecific antibody inhibits the interaction of VEGF/VEGFR2 and Dll4/Notch1, competitive inhibition ELISAs were performed using 96-well Nunc-

Immuno MaxiSorp plates with each ligand and each receptor. For the VEGF/VEGFR2 competition assays, the plates were coated with recombinant human VEGF (15 ng/well) for 16 hours at  $4^\circ\text{C}$ . Then, the wells were blocked by PBS containing 1% BSA for 2 hours at  $37^\circ\text{C}$ . Increasing concentrations of anti-VEGF (bevacizumab-similar) antibody or HD105 bispecific antibody were mixed with equal volumes of His-tagged recombinant human VEGFR2/Fc ( $1.65 \mu\text{g}/\text{ml}$ , R&D Systems). The mixtures of the antibody and VEGFR2/Fc were then transferred to the VEGF-coated wells and incubated for 2 hours at  $37^\circ\text{C}$ . The reactions were developed by adding peroxidase-conjugated anti-His6 antibody (Roche, 1:1,000) and visualized by adding TMB substrate reagent. The enzyme reactions were stopped after 6 min with 1 N sulfuric acid, and the reaction products were measured by reading the absorbance at 450–650 nm. The  $\text{EC}_{50}$  value was obtained from the dose–response curve from the experiments.

In the case of Dll4/Notch1 competition assays, the plates were coated with recombinant human Notch1 (50 ng/well) for 16 hours at  $4^\circ\text{C}$ . After blocking with PBS containing 1% BSA for 2 hours at  $37^\circ\text{C}$ , increasing concentrations (0.01 nM to 200 nM) of HD105 bispecific antibody or anti-Dll4 monoclonal antibody were mixed with equal volumes of rhDll4 ( $2.4 \mu\text{g}/\text{ml}$ ). The mixtures of the antibody and rhDll4 were then transferred to the Notch1-coated wells and incubated for 2 hours at  $37^\circ\text{C}$ . The reactions were developed by adding peroxidase-conjugated anti-His6 antibody (Roche, 1:500) and visualized by adding TMB substrate. The enzyme reactions were stopped after 6 min with 1 N sulfuric acid, and the reaction products were measured by reading the absorbance at 450–650 nm. The  $\text{EC}_{50}$  value was obtained from the dose–response curve from the experiments. In the case of mouse Dll4/Notch1 competition assays, the mouse HD105 bispecific antibody and the anti-mouse Dll4 antibody were used in the above assay format with recombinant mouse Dll4 and Notch1 (R&D Systems).

### **Inhibition of VEGF and Dll4 signaling pathways**

To determine whether the HD105 bispecific antibody inhibits both the VEGF/VEGFR2 and Dll4/Notch signaling pathways, Western blot analysis was performed using HUVECs. Six-well tissue culture plates were coated with recombinant human Dll4 ( $1 \mu\text{g}/\text{ml}$ ) diluted in bicarbonate buffer for 24 hours at  $4^\circ\text{C}$  and then washed with PBS twice. Anti-VEGF (bevacizumab-similar) antibody, anti-Dll4 monoclonal antibody, HD105 bispecific antibody, and DBZ (dibenzazepine, a chemical inhibitor of  $\gamma$ -secretase, downstream enzyme of Notch signaling) were pre-treated for 20 min prior to the seeding of HUVECs. HUVECs ( $5 \times 10^5$  cells) were plated onto the wells in growth medium for 1 day. Then, the cells were serum starved in EBM-2 medium (Lonza) containing 0.25% FBS (Gibco) for 24 hours. Serum-starved HUVECs were stimulated with recombinant human VEGF (100 ng/ml) for 15 min. The cells were lysed in NP-40 lysis buffer with PIC (protease and phosphatase inhibitor cocktails, Pierce), and the proteins were separated on 4% to 12% Bis-Tris gels. Finally, the proteins were blotted with antibodies against cleaved Notch1, phospho-VEGFR2, total VEGFR2, phospho-ERK, total ERK (Cell signaling) and  $\beta$ -actin (Santa Cruz).

### Effects on VEGF- and Dll4-mediated cell responses

To evaluate the in vitro cell-based potency of the HD105 bispecific antibody, VEGF-induced HUVEC sprouting and proliferation and Dll4-induced Notch-1-dependent activation of luciferase in SKOV-3-RBP-J $\kappa$  luciferase cells were assayed. The HUVEC sprouting assay was performed as described below. HUVECs (400 cells per bead) were mixed with dextran-coated Cytodex 3 microcarrier beads (Sigma) in 1 ml of EGM-2 medium. Beads with HUVECs were shaken gently every 20 min for 4 hours at 37°C, then transferred to a T25 flask in 5 ml of EGM-2. After incubation for 16 hours, the HUVEC-coated beads were washed three times with 1 ml of EGM-2 and resuspended in 2 mg/ml of fibrinogen (Sigma) to obtain 300 HUVEC-coated beads/ml. The fibrinogen/bead solution (0.5 ml) was added to 0.625 units of thrombin (Sigma) in a 24-well tissue culture plate. The fibrinogen/bead solution was allowed to clot for 5 min at 25°C followed by incubation at 37°C for 20 min. EGM-2 (1 ml) was added to each well and equilibrated with the fibrin clot for 30 min at 37°C. After removal of the medium and replacement with 1 ml of fresh medium, Detroit 551 cells ( $2 \times 10^4$  cells per well) were plated on top of the clot. The medium was changed every 3 days with appropriate antibodies for 15 days, and sprout formation was imaged using an inverted microscope (Eclipse TS100, Nikon). Each sprout was quantitated by counting the number of sprouts per bead.

In proliferation assays, HUVECs were plated on 100 mm plates and cultured to reach 80% sub-confluence, then serum starved in starvation medium (EBM-2 + 0.25% FBS) for 24 hours. After serum starvation, the HUVECs were trypsinized and diluted to  $6 \times 10^4$  cells/ml in the starvation medium. A total of 3,000 HUVECs were seeded into each well. Anti-VEGF (bevacizumab-similar) antibody or HD105 bispecific antibody was serially diluted from 16.5 nM to 0.32 nM in the starvation medium containing human VEGF (100 ng/ml). Then, HUVECs were immediately treated with 50  $\mu$ l of prepared antibodies at each concentration in triplicate. After an additional 72 hours of incubation at 37°C, HUVEC proliferation was detected by adding 10  $\mu$ l of CCK-8 reagent (Dojindo) followed by incubation for 5 hours at 37°C. Absorbance at 450 nm was measured using a microplate reader (Molecular Devices).

To test whether the HD105 bispecific antibody inhibits Dll4-induced Notch-1-dependent activation, SKOV-3 cells (ATCC) were infected with a lentiviral particle expressing RBP-J $\kappa$  reporter and Renilla luciferase reporter (Qiagen) that is responsive to Dll4/Notch signaling. Recombinant human Dll4 (100 ng/well) was coated onto white 96-well plates (Costar) for 24 hours at 4°C. The HD105 bispecific antibody or anti-Dll4 monoclonal antibody was serially diluted 3-fold from 30 nM to 0.002 nM and then added to each well. Engineered SKOV-3 RBP-J $\kappa$ -luciferase cells were added to the wells and incubated for 24 hours. Luciferase activity was measured using a One-Glo luciferase assay kit (Promega) and HTRF Luminescence detector (BMG Labtech).

### Animal studies and immunohistochemical analysis

To evaluate the in vivo efficacy of the HD105 bispecific antibody, tumor growth was measured after treatment with

the mouse version of HD105 bispecific antibody, anti-VEGF (bevacizumab-similar) antibody or anti-mouse Dll4 monoclonal antibody in A549 human lung and SCH human gastric cancer xenograft models. All procedures for animal studies were approved by the Institutional Animal Care and Use Committee. Balb/c athymic nude mice (8-week-old female, Charles River Japan) were injected subcutaneously in the flank area with A549 and SCH cancer cells ( $1 \times 10^7$  cells/head). When the tumors were grown to an average volume of 150–200 mm<sup>3</sup>, the mice were divided into homogenous groups (6–7 mice/group) and treated with the mouse version of HD105 bispecific antibody (3.25 mg/kg; same molar concentration with single-antigen-targeting antibodies), anti-VEGF (bevacizumab-similar) antibody or anti-mouse Dll4 monoclonal antibody (2.5 mg/kg) twice per week (A549) or once a week (SCH) by intraperitoneal injection. Tumor size was measured twice per week using a caliper and then calculated by the formula (length [mm])  $\times$  (width [mm])<sup>2</sup>  $\times$  0.5. When the average tumor size of the control group reached 1,500–2,000 mm<sup>3</sup>, the treatment was stopped and the mice were sacrificed to measure the tumor weight. Some mice were perfused with 4% paraformaldehyde in PBS for the further analysis of tumors.<sup>9,10</sup> A dose-dependent response study of HD105 bispecific antibody (0.361, 1.083, 3.25, and 6.5 mg/kg; once per week, intraperitoneal injection) was performed in the SCH gastric cancer xenograft model. The in vivo efficacy of the HD105 bispecific antibody (6.5 mg/kg; once a week, intraperitoneal injection) on the tumor progression of other human gastric cancers was confirmed using MKN-74, SNU-5 and SNU-16 cancer xenograft models.

To investigate whether the treatment with HD105 bispecific antibody affects tumor angiogenesis and tumor cell survival, A549 and SCH tumor sections were analyzed by immunohistochemical staining. For immunohistochemical analysis, SCH tumors were removed from some mice after cardiac perfusion and embedded in OCT solution (SAKURA) to produce frozen tumor blocks. Functional patent tumor vessels were stained by FITC-labeled *Lycopersicon esculentum* (tomato) lectin (Vector Laboratories), which was intravenously injected (50  $\mu$ l, circulation for 3 min) prior to perfusion of the mice.<sup>9,10</sup> The frozen tumors were sectioned (10  $\mu$ m or 20  $\mu$ m; Microm HM505N, Thermo) and permeabilized with washing buffer (PBS buffer containing 0.03% Triton X-100) for 1 hour, then blocked with 5% normal goat (Gibco) serum in the washing buffer. Tumor vessels, vascular basement membrane, and vascular pericytes were stained with rat anti-mouse CD31 (1:250, BD), rabbit anti-mouse type IV collagen antibody (1:500, Millipore), and rabbit anti-mouse NG2 antibody (1:500, Millipore), respectively. Apoptotic cells in the tumors were stained with rabbit anti-mouse/human activated caspase-3 antibody (1:500, R&D Systems). After being washed four times, the sections were stained for each secondary antibody, Alexa-568- or Alexa-488-conjugated goat anti-rat IgG (1:250, Life Technologies) or Alexa-568- or Alexa-488-conjugated goat anti-rabbit IgG (1:250, Life Technologies). Stained tumors were mounted with Vectashield (Vector Laboratories) containing DAPI (4',6-diamidino-2-phenylindole), and digital

images of the tumors were captured by a Zeiss fluorescent microscope (Axiovert 200M, Carl Zeiss) with a camera (AxioCam, Carl Zeiss). Digital fluorescence images were analyzed using ImageJ software (version: 1.46r, NIH).

### Mouse PK studies

To compare the PK profiles and parameters of the HD105 bispecific antibody with anti-Dll4 monoclonal antibody, the HD105 bispecific antibody (3.25 mg/kg) and anti-Dll4 monoclonal antibody (2.5 mg/kg) were intraperitoneally injected into BALB/c mice (n=5). Mouse serum was harvested at different time points (1, 2, 6, 24, 48, 96, 168, 216, 264, and 336 hours), and then the concentration of each antibody was measured by the Dll4-binding ELISA method. The PK parameters including  $T_{max}$ ,  $C_{max}$ ,  $AUC_{0-24}$ ,  $T_{1/2}$  of each antibody were determined based on non-compartment model.

### Stability of antibodies

To determine the stability of the HD105 bispecific antibody, HD105 (20 mg/ml) in histidine buffer including NaCl, arginine and trehalose was stored at 4°C, 25°C, or 40°C for 4 weeks, and then was analyzed by SEC-HPLC, SDS-PAGE (silver staining kit, Elpis-Biotech), and DACE after 1 week, 2 weeks, and 4 weeks.

### Statistics

Values are expressed as the means  $\pm$  SE. The significance of differences between group means was assessed by ANOVA followed by the Bonferroni test for multiple comparisons ( $P < 0.05$  values were considered significant).

### Disclosure of potential conflicts of interest

All authors are employees of Hanwha Chemical in the Biologics Unit.

### Funding

This work was supported by the Industrial Strategic Technology Development Program (Program number: 10035604; Program title: Anti-cancer bi-specific antibody with regulation of angiogenesis) funded by the Ministry of Trade, Industry and Energy (MOTIE, Korea) & Korea Evaluation Institute of Industrial Technology (KEIT).

### References

- Neufeld G, Cohen T, Gengrinovitch S, Poltorak Z. Vascular endothelial growth factor (VEGF) and its receptors. *FASEB J* 1999; 13:9-22; PMID:9872925
- Meadows KL, Hurwitz HI. Anti-VEGF therapies in the clinic. *Cold Spring Harb Perspect Med* 2012; 2:a006577; PMID:23028128; <http://dx.doi.org/10.1101/cshperspect.a006577>
- Casak SJ, Fashoyin-Aje I, Lemery SJ, Zhang L, Jin R, Li H, Zhao L, Zhao H, Zhang H, Chen H, et al. FDA Approval Summary: Ramucirumab for Gastric Cancer. *Clin Cancer Res* 2015; 21:3372-6; PMID:26048277; <http://dx.doi.org/10.1158/1078-0432.CCR-15-0600>
- Trichonas G, Kaiser PK. Aflibercept for the treatment of age-related macular degeneration. *Ophthalmol Ther.* 2013; 2:89-98; PMID:25135809; <http://dx.doi.org/10.1007/s40123-013-0015-2>
- Bergers G, Hanahan D. Modes of resistance to anti-angiogenic therapy. *Nat Rev Cancer* 2008; 8:592-603; PMID:18650835; <http://dx.doi.org/10.1038/nrc2442>
- Abdullah SE, Perez-Soler R. Mechanisms of resistance to vascular endothelial growth factor blockade. *Cancer* 2012; 118:3455-67; PMID:22086782; <http://dx.doi.org/10.1002/cncr.26540>
- Paez-Ribes M, Allen E, Hudock J, Takeda T, Okuyama H, Vinals F, Inoue M, Bergers G, Hanahan D, Casanovas O. Antiangiogenic therapy elicits malignant progression of tumors to increased local invasion and distant metastasis. *Cancer Cell* 2009; 15:220-31; PMID:19249680; <http://dx.doi.org/10.1016/j.ccr.2009.01.027>
- Ebos JM, Lee CR, Cruz-Munoz W, Bjarnason GA, Christensen JG, Kerbel RS. Accelerated metastasis after short-term treatment with a potent inhibitor of tumor angiogenesis. *Cancer Cell* 2009; 15:232-9; PMID:19249681; <http://dx.doi.org/10.1016/j.ccr.2009.01.021>
- Hashizume H, Falcón BL, Kuroda T, Baluk P, Coxon A, Yu D, Bready JV, Oliner JD, McDonald DM. Complementary actions of inhibitors of angiopoietin-2 and VEGF on tumor angiogenesis and growth. *Cancer Res* 2010; 70:2213-23; PMID:20197469; <http://dx.doi.org/10.1158/0008-5472.CAN-09-1977>
- You WK, Sennino B, Williamson CW, Falcón B, Hashizume H, Yao LC, Aftab DT, McDonald DM. VEGF and c-Met blockade amplify angiogenesis inhibition in pancreatic islet cancer. *Cancer Res* 2011; 71:4758-68; PMID:21613405; <http://dx.doi.org/10.1158/0008-5472.CAN-10-2527>
- Gale NW, Dominguez MG, Noguera I, Pan L, Hughes V, Valenzuela DM, Murphy AJ, Adams NC, Lin HC, Holash J, et al. Haploinsufficiency of delta-like 4 ligand results in embryonic lethality due to major defects in arterial and vascular development. *Proc Natl Acad Sci U S A* 2004; 101:15949-54; PMID:15520367; <http://dx.doi.org/10.1073/pnas.0407290101>
- Noguera-Troise I, Daly C, Papadopoulos NJ, Coetsee S, Boland P, Gale NW, Lin HC, Yancopoulos GD, Thurston G. Blockade of Dll4 inhibits tumour growth by promoting non-productive angiogenesis. *Nature* 2006; 444:1032-7; PMID:17183313; <http://dx.doi.org/10.1038/nature05355>
- Ridgway J, Zhang G, Wu Y, Stawicki S, Liang WC, Chantry Y, Kowalski J, Watts RJ, Callahan C, Kasman I, et al. Inhibition of Dll4 signalling inhibits tumour growth by deregulating angiogenesis. *Nature* 2006; 444:1083-7; PMID:17183323; <http://dx.doi.org/10.1038/nature05313>
- Kuhnert F, Kirshner JR, Thurston G. Dll4-Notch signaling as a therapeutic target in tumor angiogenesis. *Vasc Cell* 2011; 3:20; PMID:21923938; <http://dx.doi.org/10.1186/2045-824X-3-20>
- Sainson RC, Harris AL. Anti-Dll4 therapy: can we block tumour growth by increasing angiogenesis? *Trends Mol Med* 2007; 13:389-95; PMID:17822956; <http://dx.doi.org/10.1016/j.molmed.2007.07.002>
- Miles KM, Seshadri M, Ciamporero E, Adelaiye R, Gillard B, Sotomayor P, Attwood K, Shen L, Conroy D, Kuhnert F, et al. Dll4 blockade potentiates the anti-tumor effects of VEGF inhibition in renal cell carcinoma patient-derived xenografts. *PLoS One* 2014; 9:e112371; PMID:25393540; <http://dx.doi.org/10.1371/journal.pone.0112371>
- Kuramoto T, Goto H, Mitsushashi A, Tabata S, Ogawa H, Uehara H, Saijo A, Kakiuchi S, Maekawa Y, Yasutomo K, et al. Dll4-Fc, an inhibitor of Dll4-notch signaling, suppresses liver metastasis of small cell lung cancer cells through the downregulation of the NF- $\kappa$ B activity. *Mol Cancer Ther* 2012; 11:2578-87; PMID:22989420; <http://dx.doi.org/10.1158/1535-7163.MCT-12-0640>
- Jenkins DW, Ross S, Veldman-Jones M, Foltz IN, Clavette BC, Manchulenko K, Eberlein C, Kendrew J, Petteruti P, Cho S, et al. MEDI0639: a novel therapeutic antibody targeting Dll4 modulates endothelial cell function and angiogenesis in vivo. *Mol Cancer Ther* 2012; 11:1650-60; PMID:22679110; <http://dx.doi.org/10.1158/1535-7163.MCT-11-1027>
- Li JL, Sainson RC, Oon CE, Turley H, Leek R, Sheldon H, Bridges E, Shi W, Snell C, Bowden ET, et al. DLL4-Notch signaling mediates tumor resistance to anti-VEGF therapy in vivo. *Cancer Res* 2011; 71:6073-83; PMID:21803743; <http://dx.doi.org/10.1158/0008-5472.CAN-11-1704>

20. Kuhnert F, Chen G, Coetzee S, Thambi N, Hickey C, Shan J, Kovalenko P, Noguera-Troise I, Smith E, Fairhurst J, et al. DLL4 Blockade in Stromal Cells Mediates Antitumor Effects in Preclinical Models of Ovarian Cancer. *Cancer Res* 2015; 75:4086-96; PMID:26377940; <http://dx.doi.org/10.1158/0008-5472.CAN-14-3773>
21. Hoey T, Yen WC, Axelrod F, Basi J, Donigian L, Dylla S, Fitch-Bruhns M, Lazetic S, Park IK, Sato A, et al. DLL4 blockade inhibits tumor growth and reduces tumor-initiating cell frequency. *Cell Stem Cell* 2009; 5:168-77; PMID:19664991; <http://dx.doi.org/10.1016/j.stem.2009.05.019>
22. Marvin JS, Zhu Z. Recombinant approaches to IgG-like bispecific antibodies. *Acta Pharmacol Sin* 2005; 26:649-58; PMID:15916729; <http://dx.doi.org/10.1111/j.1745-7254.2005.00119.x>
23. Michaelson JS, Demarest SJ, Miller B, Amatucci A, Snyder WB, Wu X, Huang F, Phan S, Gao S, Doern A, et al. Anti-tumor activity of stability-engineered IgG-like bispecific antibodies targeting TRAIL-R2 and LTbetaR. *mAbs* 2009; 1:128-41; PMID:20061822; <http://dx.doi.org/10.4161/mabs.1.2.7631>
24. Milenic DE, Yokota T, Filpula DR, Finkelman MA, Dodd SW, Wood JF, Whitlow M, Snoy P, Schlom J. Construction, binding properties, metabolism, and tumor targeting of a single-chain Fv derived from the pancarcinoma monoclonal antibody CC49. *Cancer Res* 1991; 51:6363-71; PMID:1933899
25. Zhou Y, Goenaga AL, Harms BD, Zou H, Lou J, Conrad F, Adams GP, Schoeberl B, Nielsen UB, Marks JD. Impact of intrinsic affinity on functional binding and biological activity of EGFR antibodies. *Mol Cancer Ther* 2012; 11:1467-76; PMID:22564724; <http://dx.doi.org/10.1158/1535-7163.MCT-11-1038>
26. Clarke JM, Hurwitz HI. Understanding and targeting resistance to anti-angiogenic therapies. *J Gastrointest Oncol* 2013; 4:253-63; PMID:23997938; <http://dx.doi.org/10.3978/j.issn.2078-6891.2013.036>
27. Yen WC, Axelrod F, Bond C, Cain J, Chartier C, Fischer M, Ma S, Meisner R, Raval J, Shah J. Dual targeting of DLL4 and VEGF signaling by a novel bispecific antibody inhibits tumor growth and reduces cancer stem cell frequency. *AACR Annual Meeting 2014*; 2014 April 5-9; San Diego, CA
28. Gurney AL, Sato AK. inventors; Oncomed Pharmaceuticals, Inc., assignee. Method for making heteromultimeric molecules. United States patent US2011/0123532 A1. 2011 May 26
29. Yang HY, Kang KJ, Chung JE, Shim H. Construction of a large synthetic human scFv library with six diversified CDRs and high functional diversity. *Mol Cells* 2009; 27:225-35; PMID:19277506; <http://dx.doi.org/10.1007/s10059-009-0028-9>
30. Ki MK, Kang KJ, Shim H. Phage display selection of EGFR-specific antibodies by capture-sandwich panning. *Biotechnology and Bio-process Engineering* 2010; 15:152-6; <http://dx.doi.org/10.1007/s12257-009-3080-6>